Flora 272 (2020) 151693

Contents lists available at ScienceDirect

Flora

journal homepage: www.elsevier.com/locate/flora

Ontogenesis and responses to shading of *Attalea vitrivir* (Arecaceae) eophyll

Isabella Renata Gomes da Cunha [a], Leonardo Monteiro Ribeiro [a,*], Maria Olívia Mercadante-Simões [a], Levi Fraga Pajehú [b], Paulo Sérgio Nascimento Lopes [b], Márcio Antônio Silva Pimenta [a]

[a] Departamento de Biologia Geral, Universidade Estadual de Montes Claros, 39401-089, Montes Claros, Minas Gerais, Brazil
[b] Instituto de Ciências Agrárias, Universidade Federal de Minas Gerais, 39404-547, Montes Claros, Minas Gerais, Brazil

ARTICLE INFO

Keywords:
Leaf anatomy
Palm seedlings
Photosynthesis
Seedling establishment
Shading

ABSTRACT

The eophylls (first photosynthetic leaves) of palm trees play crucial roles in seedling establishment, although information concerning their development and ecophysiology remain scarce. This work sought to evaluate eophyll development and the effects of shading on young plants of the neotropical oil palm *Attalea vitrivir*. Eophyll ontogenesis was characterized, and the effects of shading levels (0, 58, 73 and 93%) on their anatomy, histochemistry, and seedling development where evaluated. Photosynthetic responses were compared between plants exposed to full sunlight or shade. After germination, the cotyledonary petiole elongates downward, which promotes the burial of the vegetative axis. Two eophylls are formed by the apical meristem, and they develop a short petiole and a much-folded blade that grows through the action of a basal meristem. The eophylls emerge below soil level and show a typical leaf structure and an intense and diverse vasculature. Shading levels do not affect blade tissue thicknesses, stomatal density, or the presence of primary and secondary metabolic compounds. A low photosynthetic performance under shade conditions is compensated by greater blade growth, so that plant development is not affected by shading. The ontogenesis of *A. vitrivir* eophylls below the soil surface and their response to shading contributes to seedling establishment and the adaptation of the species to seasonal and anthropized environments.

1. Introduction

Palm trees develop specialized types of initial leaves that play crucial roles in seedling establishment (Gunawardena and Dengler, 2006; Tillich, 2007). The first photosynthetic leaves (eophylls) are distinct from definitive leaves (metaphylls) and show wide structural diversity among Arecaceae taxa (Henderson, 2006). In-depth studies focusing on the ontogenesis, structure, and functionality of palm eophylls have been scarce (Henderson, 2006; Dransfield et al., 2008), but can contribute to the expansion of our knowledge concerning the adaptations of different species to different environments and provide useful information for palm propagation and cultivation efforts.

Light is an important modulator of plant development (Poorter, 2001; Markesteijn et al. 2007). The light regimes to which plants are exposed can influence biomass production (Poorter, 2001; Gatti et al., 2011), the synthesis of primary and secondary metabolites (Dickison, 2000; Agati et al., 2011), and leaf anatomy (Araus and Hogan, 1994; Markesteijn et al., 2007; Pereira et al., 2013). Most young palm plants are shade-tolerant and grow in the understories of tropical forests (Dransfield et al., 2008; Corrêa et al., 2019). Young plants of pioneer species that are adapted to colonizing open environments, on the other hand, are commonly exposed to high light intensities and water deficits and develop peculiar structures and distinct physiological processes that have not yet been closely studied (Araus and Hogan, 1994; Orozco-Segovia et al., 2003; Dransfield et al., 2008).

Attalea vitrivir Zona is a palm tree endemic to the Cerrado (neotropical savanna) biome in central Brazil (Lorenzi et al., 2010) and is therefore adapted to a highly seasonal climate with pronounced water deficits occurring for several months during the austral winter (Guedes et al., 2015). The species demonstrates a pioneer-behavior for occupying open areas close to water courses, where it can form dense monodominant populations (Neves et al., 2013). *A. vitrivir* has social

Key Message: The patterns of eophyll development and leaf adaptations to different levels of shading contribute to seedling establishment and the reproductive success of the palm *Attalea vitrivir*.

* Corresponding author. Tel.: 55 38 3229-8154, Fax: 55 38 3229-8180.
E-mail address: leonardo.ribeiro@unimontes.br (L.M. Ribeiro).

https://doi.org/10.1016/j.flora.2020.151693
Received 13 April 2020; Received in revised form 22 July 2020; Accepted 31 August 2020
Available online 3 September 2020

importance to human populations as a food source and for construction and handicraft purposes (Lorenzi et al., 2010). It also represents a potential source of biomass for charcoal production for use in steel mills (Teixeira, 2008) and the production of biofuels (Santos et al., 2007). Information concerning seedling development in the species is still scarce (Neves et al., 2013; Guedes et al., 2015), however, but would contribute to the expansion of our knowledge concerning its reproduction and propagation.

The present work was therefore designed to characterize the ontogenesis and structure of *A. vitrivir* eophyll, evaluate their responses to shading, and respond to the following questions: i) how does the eophyll develop, and what are the particularities of its anatomy? ii) How does eophyll development and their responses to shading (leaf anatomy, the production of primary and secondary metabolites, and photosynthetic activity) contribute to the survival of the species in the environments in which it occurs?

2. Materials and methods

2.1. Plant material and preliminary procedures

A. vitrivir fruits were obtained (after natural abscission) from a natural population growing in the Rio Pandeiros Environmental Protection Area in the municipality of Januária, in northern Minas Gerais State, Brazil (15°26'10''S, 44°04'44''W). The seeds were removed from the fruits using an ax and subsequently culled, discarding damaged propagules, or those with symptoms of microbial contamination. The selected seeds were then packed in plastic bags and stored in a dry and ventilated area for up to 60 days, until evaluations were made.

2.2. Morphologic evaluations of the seedlings

The seeds were immersed in a 6% NaClO solution for 15 minutes, and then rinsed three times in tap water. The operculum was removed to promote germination, and the seeds were sown into polyethylene trays and covered with vermiculite moistened with distilled water (up to 70% of its retention capacity), and then held in a germinator at 30°C (Neves et al., 2013). Germinated seeds were planted in polyethylene sacks (3 L capacity) containing a mixture of clay soil and sand (3:1), and then kept in a greenhouse for 60 days. Five plants were evaluated daily, using a stereomicroscope, for the first 10 days, and then every five days. The morphology of the cotyledonary petiole, cotyledonary petiole tube, leaf sheaths, roots and eophylls has been described, according to the terminology used by Neves et al. (2013).

2.3. Eophyll ontogenesis

The distal portions of five cotyledonary petioles (with the embryonic axis inside) were obtained from embryos before planting, and then again one and three days after sowing. Samples from the petiole tube region (containing the vegetative axis) were obtained from five seedlings at seven, 14, 21 and 28 days after sowing. The material was fixed in Karnovsky solution (Karnovsky, 1965) for 24 h, dehydrated in an ethanol series (Jensen 1962), and embedded in cold (2-hydroxyethyl)-methacrylate (Leica Microsystem Inc., Heidenbeg, Germany) Paiva et al., 2011. Cross- and longitudinal sections (5 μm thick) were obtained using a rotating microtome (Atago, Tokyo, Japan), stained with 0.05% (w/v) toluidine blue in 0.1 M acetate buffer pH 4.7 (O'Brien et al. 1964, modified), and mounted on slides in acrylic resin (Itacril, Itaquaquecetuba, Brazil). Photographic documentation was performed using a photomicroscope (AxioVision LE/AxioCam MRc, Zeiss, Oberkochen, Germany).

The cotyledonary petiole tubes of three seedlings (after 14 and 28 days of cultivation) were submitted to clearing. The tubes were sectioned longitudinally, fixed in 50% ethanol for 24 hours, and dehydrated in series to 70% ethanol. The material was then immersed in a 5% NaOH solution at 60°C, stained with fuchsin for 24 hours, and held in 95% ethanol for 30 days (Fuchs, 1963). Photographic documentation was performed using a digital camera coupled to a stereomicroscope (Stemi 305 / Axiocam ICc 3, Zeiss, Jena, Germany).

2.4. Cultivation under different degrees of shading

Seedlings grown in polyethylene sacks (as described above for the morphological evaluations) that had eophyll blades with average lengths and widths of 18 and 2 cm, respectively, were transferred (in groups of four) to full sunlight as well as to shaded environments (58%, 73% and 93% shade). The shading levels of 58% and 73% were obtained by covering the plants with black polypropylene mesh; 93% shading was obtained using cotton cloth extended 60 cm above ground level. Light intensity measurements were made using a digital light meter (MLM-1011, Minipa, São Paulo, Brazil) between the hours of 12:00 and 13:00, for 30 days. The measurements were carried out in full sunlight and under the light shades. Shading levels were calculated considering the proportion of light reduction between full sunlight and under the shading material. A block design was used, with five replicates (blocks) of four plants each. The plants were cultivated for 18 months with daily irritation that raised the substrate to its water retention capacity.

2.5. Anatomical characterization of the eophyll

Five plants grown for 18 months in full sunlight and under 93% shade conditions were chosen at random, and histological cross-sections and paradermic sections of the median region of the most developed eophylls were evaluated (as described above for ontogenesis evaluations). Additionally, paradermic sections were subjected to clearing, as previously described above. The terminology proposed by Tomlinson et al., 2011 for palm leaves was used in the descriptions.

To evaluate the epidermal surfaces of the eophylls, fragments (approximately 1 mm^2) were removed 7 cm from the apex of the eophyll, fixed in Karnovsky solution (Karnovsky, 1965), dehydrated in an acetone series, and subjected to critical point drying (CPD 030, Balzers, Liechtenstein, Germany) using CO_2. The samples were then splutter coated with gold (Med 010 splutter coater, Balzers, Liechtenstein, Germany) and examined using a Quantum 200 scanning electron microscope (FEI Company, Eindhoven, The Netherlands) with 12-20 kV digital image captures (Robards, 1978).

2.6. Evaluations of morphological changes in response to shading

After 18 months of cultivation, plants grown under four levels of shading were removed from their containers and the lengths of their eophyll blades and petioles, petiole diameters, underground stem diameters, and the numbers and lengths of their roots were evaluated. The dry masses of the eophyll blades and petioles, and underground stems and roots were measured (using an analytical balance) after drying at 104°C for 24 h; the total plant dry mass was subsequently calculated.

2.7. Micromorphometric evaluations

The eophylls from plants grown at four different shade levels for six and 18 months were evaluated. Five histological cross sections were made per treatment in the median region of the most-developed eophyll, as described above. The sections were photographed using a digital camera (Moticam, Hong Kong, China) coupled to an optical microscope (Eclipse E-200, Nikon, Tokyo, Japan). Measurements of blade, epidermal, hypodermal, and mesophyll thicknesses were obtained using Image-Pro-Plus version 4.5 software (Media Cybernetics, Silver Spring, EUA).

Stomatal density was evaluated using 0.5 cm^2 fragments of the epidermis dissociated from the median region of the eophyll. Dissociation was performed using the Jeffrey method (Johansen, 1940,

Table 1
Morphological characteristics of *Attalea vitrivir* plants subjected to four different levels of shading for 18 months.

Characteristic	Shading (%)			
	0	58	73	93
Root length (cm)	37.9 a	34.1 a	30.9 a	25.6 b
Petiole length (cm)	6.0 b	7.0 b	8.3 a	8.3 a
Eophyll blade length (cm)	30.9 b	35.5 b	43.8 a	48.1 a
Leaf dry mass (g)	12.6 b	15.6 a	20.7 a	21.6 a

Different letters on the same line indicate significant differences by the Tukey test ($P < 0.05$).

modified). Those fragments were fixed in 50% FAA for 24 hours, dehydrated to 70% ethanol, and immersed in a 10% potassium dichromate and 10% nitric acid (v/v) solution. The epidermal faces were separated using a brush, stained with toluidine blue pH 4.7 (modified by O'Brien and McCully, 1981), and mounted on permanent slides using acrylic resin (Itacril, Itaquaquecetuba, Brazil). Stomatal densities (stomata mm^{-2}) were evaluated by photomicroscopic captures of three fields, with five replicates per treatment.

2.8. Histochemical evaluations

Plants exposed for eighteen months to full sunlight as well as to 93% shade were evaluated. The treatments were chosen due to their contrasting effects on plant morphology and development, Table 1. Histological cross sections were obtained, as described above for the micromorphometric evaluations. The sections were subjected to the following tests: lugol to detect starch (Jensen, 1962); Sudan black to detect lipids (Pearse, 1972); bromophenol blue (Mazia et al., 1953) and Xylidine-Ponceau - XP (Vidal, 1977) to detect proteins; tannic acid (Pizzolato and Lillie, 1973) for mucilage; vanillin-hydrochloric acid for tannins (Mace and Howell, 1974), p-dimethylaminocinnamaldehyde (DMACA) for flavonoids (Feucht et al., 1986; Arnous, 2002); Dittmar and Wagner reagents for alkaloids (Furr and Mahlberg, 1981); and naphthol-dimethyl-paraphenylene-diamine - NADI to detect terpenoids (David and Carde, 1964). Photographic documentation was performed as described above for the micromorphometric evaluations.

2.9. Photosynthetic responses to shading

Plants grown for one year under full sunlight or 93% shade were evaluated. The treatments were chosen due to their contrasting effects on plant morphology and development, Table 1. Leaf temperature (Tleaf), stomatal conductance (gs), transpiration (E), CO_2 assimilation (A), and internal carbon (IC) were evaluated in eight plants per treatment. Water use efficiency (WUE) was also calculated, considering the relationship between CO_2 assimilation and transpiration. The evaluations were carried out using an infra-red gas analyzer (LCpro-SD, ADC Bio-Scientific Ltd, Hoddesdon, UK), with readings being taken between 12:00 and 12:30, in the mid-third of the most developed eophyll of each plant.

2.10. Statistical analyses

Biometric, micromorphometric, and stomatal density data were subjected to the Kolmonogov-Smirnov normality test and Levene's test of homogeneity of variance. Analysis of variance was used and the means were compared using the Tukey test, at a 5% level of probability.

Fig. 1. Seedling morphology of *Attalea vitrivir*. a) Five days after sowing, seed showing protrusion of the cotyledonary petiole, with positive geotropic orientation. b) Seven days after sowing, cotyledonary petiole showing the elongation that promotes the burial of the vegetative axis inserted within the tube region (arrow). c) 10 days after sowing, cotyledonary petiole showing significant elongation and swelling in the tube region (arrow). d) 15 days after sowing, highlighting the main root emitted from the end of the cotyledonary petiole (arrow). e) 25 days after sowing, showing the cotyledonary petiole with maximum elongation and the main root. f) 35 days after sowing, showing the first leaf sheath emitted through the cotyledonary cleft. g) 45 days after sowing, showing the second leaf sheath (emitted internally to the first sheath) stretching to the soil surface. h) 60 days after sowing, highlighting the first eophyll, with its blade beginning to expand above ground level. cp, cotyledonary petiole; ro, main root; s1, first leaf sheath; s2, second leaf sheath; se; seed; tu, cotyledon tube. Scale bars = 10 mm.

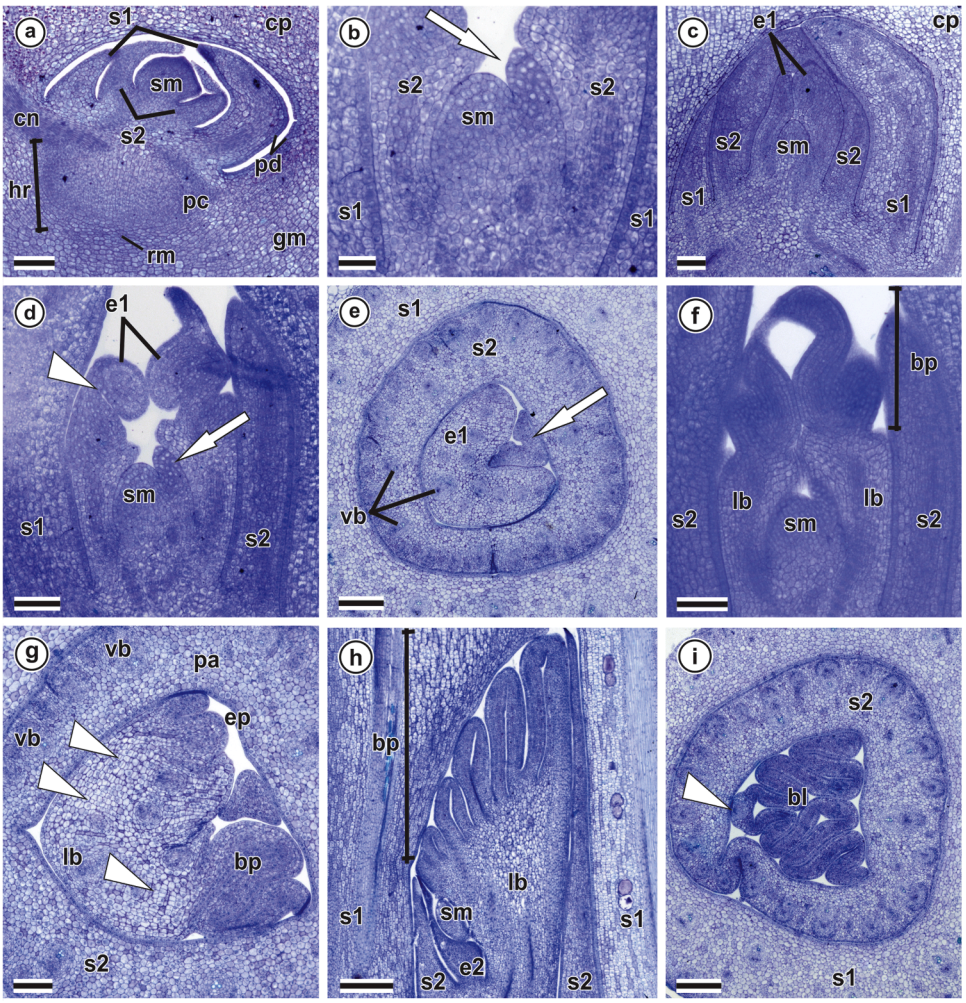

Fig. 2. Anatomy of the embryo and seedlings of *Attalea vitrivir*. Longitudinal sections (a-d, f, h). Cross sections (e, g, i). a) Embryonic axis before sowing. b) Plumule, one day after sowing, showing the initial phase of differentiation of the first eophyll from the apical meristem (arrow). c) Plumule, three days after sowing, showing the growth of the first eophyll. d-e) Stem apex, seven days after sowing, showing the formation of folds in the eophyll blade primordium (arrowhead), and the second eophyll in early development (arrows). f-g) Stem apex, 14 days after sowing, showing the differentiation of the first eophyll, with the formation of the leaf base and blade primordium (f) and numerous cell divisions in the leaf base region (g). h) Stem apex, 21 days after sowing, showing several folds formed in the blade primordium. i) Stem apex, 28 days after sowing, showing the blade of the first eophyll with many folds, highlighting the median rib (arrowhead). bp, blade primordium; cn, cotyledon node; cp, cotyledonary petiole; e1, first eophyll; e2, second eophyll; ep, epidermis; gm, ground meristem; hr, hypocotyl-radicle axis; lb, leaf base; pa, parenchyma; pc, procambium; pd, protoderm; rm, root apical meristem; sm, stem apical meristem; s1, first leaf sheath; s2, second leaf sheath; vb, vascular bundle. Scale bars: a, c, d, f, g = 100 μm; b = 50 μm; and, h, i = 200 μm.

3. Results

3.1. Seedling morphology

Germination could be confirmed by the protrusion of the cotyledonary petiole three days after sowing. A marked curvature of the petiole, with a positive geotropic orientation, was observed (Fig. 1a), and pronounced elongation for up to 10 days (Fig. 1b-c). The growth of that structure resulted in the burial of the vegetative axis (located in the swollen tube composing the distal portion of the petiole) (Fig. 1c). After 15 days of cultivation, the growth of the petiole had slowed and the main root had been emitted from its end (Fig. 1d). At 25 days of cultivation, the petiole had ceased to elongate, the cotyledon tube became expanded, and the main root had developed (Fig. 1e). At 35 days of cultivation, the emergence of the first leaf sheath (through the cotyledonary cleft, located laterally in the tube) was evident (Fig. 1f). At 45 days, the proliferation of lateral roots and the elongation of the second leaf sheath were observed (the latter emitted internally to the first, and often very close to the soil surface) (Fig. 1g). At 60 days, the eophyll had been emitted (internal to the second sheath) and had begun its expansion above the soil surface (Fig. 1h).

3.2. Eophyll ontogenesis

The embryonic axis of *A. vitrivir* is located internal to the cotyledonary petiole, has microscopic dimensions, and consists of a plumule and hypocotyl-radicle axis (Fig. 2a). The plumule is inserted in a cavity in the cotyledonary petiole and consists of an apical meristem surrounded by two tubular leaf sheaths. Those sheaths have an unistratified protoderm covering the fundamental meristem, with dispersed procambial strands. It was possible to observe the initiation of differentiation of the first eophyll from the apical meristem one day after sowing (Fig. 2b). At three days after sowing, the first eophyll showed significant elongation and had acquired a tubular conformation (Fig. 2c). At seven days after sowing, the internal region of the apex of the first eophyll showed irregular growth, creating several folds (Fig. 2d). The beginning of the development of the second eophyll could also be observed, in a pattern similar to that of the first (Fig. 2d-e), as well as the differentiation of vascular bundles in the two leaf sheaths and the first eophyll (Fig. 2e). At 14 days after sowing, two regions could be identified in the first eophyll: a tubular-shaped basal portion (leaf base) and an apex (blade primordium) with folds (Fig. 2f). The leaf base showed cells undergoing intense divisions in several planes (Fig. 2g). At 21 days after sowing, the expansion of the leaf base cells as well as blade growth were evident, with increasing numbers and extensions of the folds (Fig. 2h). At 28 days after sowing, the differentiation of the blade was evident in the apical region, with numerous folds and a median rib (Fig. 2i).

Examinations of the cleared material showed that the first eophyll develops within an intensely vascularized region (Fig. 3a). The beginning of vascular bundle differentiation in the eophyll could be seen 14 days after sowing. After 28 days of cultivation, the blade primordium was arrow-shaped, with the leaf base having a narrower conformation, with the petiole beginning to differentiate from the eophyll (Fig. 3b).

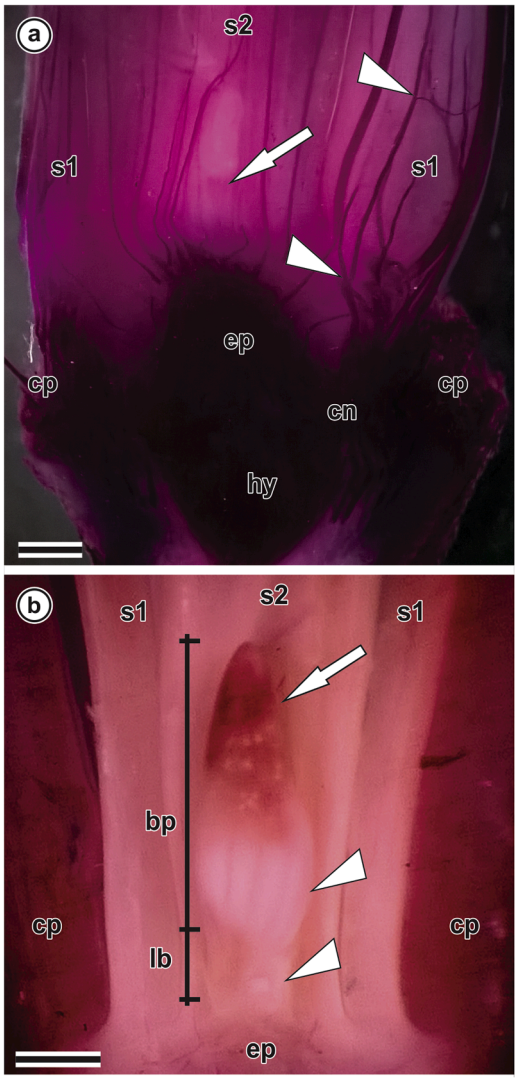

Fig. 3. Longitudinal sections of the cleared stem apex of a *A. vitrivir* seedling. a) 14 days after sowing, showing the highly vascularized regions of the hypocotyl, epicotyl, cotyledon node, and cotyledonary petiole, and highlighting ramifications in the vascular bundles of the first leaf sheath (arrowheads) and the beginning of vascularization of the first eophyll (arrow). b) After 28 days of sowing, showing the different regions of the eophyll, and highlighting the distal region with its more developed vasculature (arrow), as well as regions with poorly developed vasculature in the blade primordium and leaf base (arrowhead). bp, blade primordium; cn, cotyledon node; cp, cotyledonary petiole; ep, epicotyl; hy, hypocotyl; lb, leaf base; s1, first leaf sheath; s2, second leaf sheath; vb, vascular bundle. Scale bars = 500 μm.

The vasculature had differentiated in the distal portion of the blade primordium, while the proximal region (and the leaf base) were less differentiated, reflecting their meristematic natures.

3.3. Eophyll anatomy

Plants cultivated in full sunlight or under 93% shading throughout their development showed eophylls with a lanceolate blade and parallel venation associated with numerous folds (Fig. 4a). The longitudinal ribs were transversely connected by smaller veins (commissures) (Fig. 4a-b). The epidermis was uniseriate, and composed of ordinary cells of varying shapes and sizes (Fig. 4c-g). On the adaxial surface, in the regions of the folds, the epidermal cells took on papillary appearances (Fig. 4d). Scarce secretory trichomes formed by arciform basal cells and having short stems and globular heads, were distributed along the epidermis (Fig. 4f). The epidermal surfaces were entirely covered by abundant depositions of epicuticular wax plaques (with the exception of the stomata) (Fig. 5a-b). The leaves were amphistomatic, and the tetracytic stomata were arranged in longitudinal series in the intercostal region, with the longest axis of the guard cells oriented longitudinally (Fig. 4c, e-f). The guard cells had epicuticular crests, with longitudinal arciform subsidiary cells protruding towards both the inside of the mesophyll and outwards from the epidermis (Figs. 4e, 5c). The sub-stomatal chambers were voluminous (fig. 4e-f). A hypodermis was observed on both sides of the leaf, composed of voluminous globoid cells that constituted expansion tissue in the region of the folds, with anticlinally elongated cells (Fig. 4d-e). Bundles of sclerenchymatous fibers were interspersed in the midst of the hypodermal cells, occurring more frequently on the adaxial surface (Fig. 4d-f). The mesophyll was homogeneous and compact and composed of from four to five layers of globular parenchyma cells, with the presence of voluminous idioblasts with thin walls containing raphides immersed in a mucilaginous matrix (Fig. 4e-f).

In addition to being dense (Fig. 4b), the vasculature showed diverse conformations (Fig. 6a-d). The commissures occupied about one third of the blade thickness, with vessel elements having helical thickenings and evident sieve tube elements (Fig. 4g). Three principal types of vascular bundles with longitudinal arrangements could be identified, all of which were surrounded by parenchymal and sclerenchyma sheaths (Fig. 4h). The largest vascular bundles had sheaths in contact with both faces of the epidermis, isolated poles of phloem, and a single thick metaxylem vessel element (Fig. 6a-b); stegmata (spherical siliceous bodies) arranged in longitudinal rows were associated with the outer fibers of the sclerenchyma sheaths (Fig. 4h-i). The intermediate vascular bundles had the sheaths associated (or not) with one of the epidermal faces, diameters greater than half the mesophyll thickness, undivided phloem, and more than one thick metaxylem vessel element (Fig. 6c). The smaller vascular bundles had sheaths associated (or not) with the epidermis, diameters less than half the thickness of the mesophyll, undivided phloem, and lacked thick metaxylem vessel elements (Fig. 6d).

3.4. Morphological responses to shading

No responses to shading variations were observed for: the total dry mass of the plants (Mean = 55.0 g, P = 0.36), their roots (Mean = 21.3 g, P = 0.37), underground stems (Mean = 9.6 g, P = 0.60), or leaf petioles (Mean = 6.5 g, P = 0.093); or the numbers of roots (Mean = 4.3 cm, P = 0.085), the lengths and diameters of the underground stems (Mean: 2.6 cm, P = 0.95 and Mean = 2.0 cm, P = 0.81 respectively), or the diameters of petioles (Mean= 3.6 cm, P = 0.93). There were significant differences between treatments, however, in terms of root, petiole, and leaf blade lengths (Table 1). Greater shading conditions resulted in root length reductions, and generally greater leaf development, especially in terms of their lengths and dry masses.

3.5. Effects of shading on eophyll micromorphometry

Stomatal density on both sides of the epidermis, leaf blade thickness, as well as all of the micromorphometric characteristics evaluated, increased over time (Table 2). The different variation in shading tested, however, did not affect any of the characteristics evaluated.

3.6. Effects of shading on eophyll histochemistry

The different levels of shading did not affect the presence of primary or secondary metabolic compounds in the eophyll blade. The results obtained from eophylls developed in full sun are shown in Fig. 7a-g. Among primary compounds, where accumulations of starch (Fig. 7a), proteins (Figs. 7b-c), and mucilage (Fig. 7d) in the mesophyll cells. Among secondary metabolic compounds, flavonoids (Fig. 7e) and alkaloids were found in idioblasts that were widely distributed throughout the mesophyll (Fig. 7f), as well as terpenoids in the form of droplets in

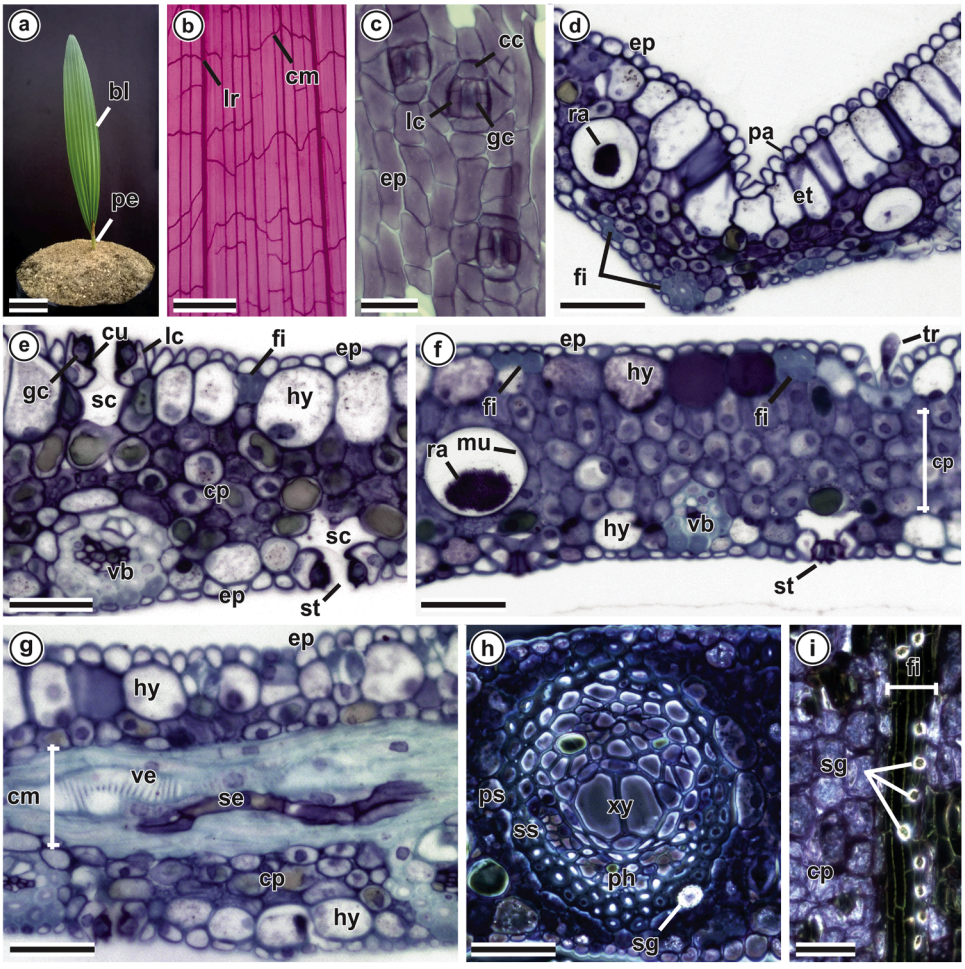

Fig. 4. Morphology and anatomy of the *Attalea vitrivir* eophyll**.** Paradermic sections (b-c). Cross sections (d-h). Longitudinal section (i). a) Eophyll in a plant after three months of development, showing the short petiole and lanceolate and folded blade. b) Cleared blade fragment showing longitudinal ribs connected transversely by commissures. c) Adaxial face of the epidermis showing tetracytic stomata. d) Fold region of the blade, showing the papillary epidermis, expansion tissue, and idioblasts with raphides. e) Flat region of the blade, highlighting the structures of the stomata and hypodermis. f) Flat region of the blade, showing trichomes, the homogeneous mesophyll, and idioblasts with raphides. g) Flat region of the blade, showing a transversal vascular bundle (commissure) with vessel elements with scalariform thickenings and sieve tube elements. h) Large-caliber vascular bundle, showing vascular tissue surrounded by a parenchyma sheath (outermost) and a sclerenchyma sheath with globoid stegmata. i) Detail of the sclerenchyma sheath of the vascular bundle, showing the distribution of stegmata associated with external fibers. bl, blade; cc, transverse cell; cm, commissure (transversal vascular bundle); cp; chlorophyll parenchyma; cu, cuticle; ep, ordinary epidermal cell; et, expansion tissue; fi, fibers; gc, guard cell; hy, hypodermis; lc, longitudinal cell; mu, mucilage; pa, papillary epidermal cell; pe, petiole; ph, phloem; ps, parenchymal sheath; ra, raphides; sc, sub-stomatal chamber; se, sieve tube element; sg, stegmata; ss, sclerenchyma sheath; st, stoma; tr, trichome; vb, vascular bundle; ve, vessel element; xy, xylem. Scale bars: a = 5 cm; b = 4 mm; c = 100 μm; d-h = 40 μm; i = 100 μm.

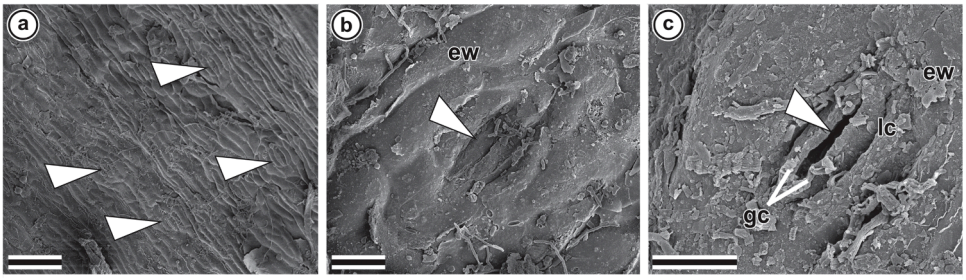

Fig. 5. Frontal image of the adaxial epidermal surface of an *Attalea vitrivir* eophyll, obtained by SEM. a) Epidermal surface covered with epicuticular wax plates, highlighting the location of the stomata (arrowheads). b) Detail of a closed stomata (arrowhead) surrounded by abundant deposits of epicuticular wax. c) Detail of an open stomata, highlighting the ostiole (arrowhead). ew, epicuticular wax; gc, guard cells; lc, longitudinal subsidiary cell. Scale bars: a = 50 μm; b-c = 10 μm

the cytoplasm of expansion tissue and epidermal cells (Fig. 7g).

3.7. Photosynthetic responses to shading

After six months of cultivation, it was found that Tleaf, g_s, E, A, and WUE were higher under conditions of full sunlight as compared to 93% shading (Fig 8a-d, f). CO_2 assimilation (A) was found to be 2.1 times greater in the eophylls of plants grown in full sunlight than under 93% shading (Fig 8d). There was no significant difference between the treatments in relation to IC (Fig. 8e).

4. Discussion

4.1. Eophyll development patterns and structures

This paper represents the first detailed description of eophyll development in *Attalea* Kunth. The elongation of the cotyledonary petiole after seed germination promotes the burial of the vegetative axis, so that the ontogenesis of the roots, leaf sheaths, and eophylls occur several centimeters below the soil surface. The positive geotropic growth of the cotyledonary petiole is associated with a development

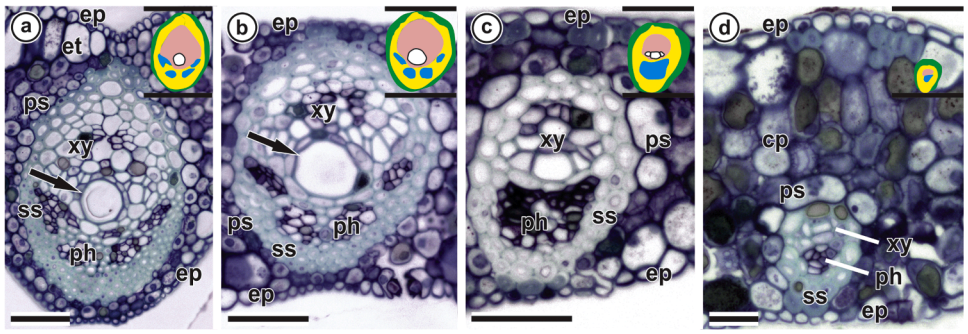

Fig. 6. Anatomy (cross sections) of the vascular bundles in the eophyll of *Attalea vitrivir*. a) Large caliber bundle associated with the region of the blade fold, with a thick metaxylem vessel element (arrow) and phloem divided into four poles. b) Large caliber bundle associated with the flat region of the blade, with a thick metaxylem vessel element (arrow) and phloem divided into four poles. c) Medium caliber bundle, with three thick metaxylem vessel elements and an undivided phloem. d) Small bundle associated with the epidermis. In the diagrams in the upper right corner: black = adaxial or abaxial face of the epidermis; green = parenchymal sheath; yellow = sclerenchyma sheath; blue = phloem; pink = xylem, white = metaxylem vessel element. cp, chlorophyll parenchyma; ep, epidermis; et, expansion tissue; ps, parenchymal sheath; ph, phloem; ss, sclerenchyma sheath; xy, xylem. Scale bars: a-c = 50 μm; d = 20 μm.

Table 2
Micromorphometric characteristics (averages obtained under full sunlight and 93% shading conditions) of the eophylls of *A.vitrivir* plants grown for 18 months.

Characteristic	6 months		18 months	
	Thickness (μm)	Density (n° mm^{-2})	Thickness (μm)	Density (n° . mm^{-2})
Stomata - adaxial		24.9 b		36.0 a
Stomata - abaxial		54.2 b		78.5 a
Blade	105.2 b		135.2 a	
Epidermis - adaxial	6.1 b		7.0 a	
Epidermis - abaxial	5.9 b		6.4 a	
Hypodermis – adaxial	20.2 b		26.3 a	
Hypodermis - abaxial	15.3 b		18.4 a	
Mesophyll	57.7 b		77.5 a	

Different letters on the same line indicate significant differences by the Tukey test (P< 0.05).

pattern known as remote tubular, sensu Martius (Henderson, 2006; Xiao et al., 2019), which is typical of species of the genera *Attalea* (Souza et al., 2000) and *Syagrus* Mart. (Bernacci et al., 2008). The eophyll of *A. vitrivir* shows slow but continuous development, and it consists of a petiole and a blade with several folds. The leaf first appears as a dome in the stem apical meristem, and continuously expands through the activity of its basal meristem – so that the most differentiated tissues are positioned in progressively more distal regions.

Palm taxa show different eophyll development patterns, which gives taxonomic value to the structure of that organ (Gunawardena and Dengler, 2006; Henderson, 2006). The structure of the *A. vitrivir* eophyll shares characteristics with other species of the Attaleinae subtribe (such as *Allagoptera leucocalyx* Kuntze, *Jubaea chilensis* Baill., *Syagrus coronata* Becc., and *Voanioala gerardii* J. Dransf.), including the prismatic shapes of their epidermal cells, tetracyclic stomata, a single-layered hypodermis, scarce trichomes, and the presence of stegmata associated with the sclerenchyma fibers of the vascular bundles (Henderson, 2006). It is important to note that while a predominantly homogeneous mesophyll is not a descriptive characteristic of the group. Useful characters for the distinction of the *A. vitrivir* eophyll described in the present work include stomatal density (Table 2), the distribution patterns of the bundles of non-vascular fibers, idioblasts containing raphides (Fig. 4 d-f) and, especially, variations in vascular bundle sizes, their position in the mesophyll, and phloem and metaxylem characteristics (Fig. 6a-d).

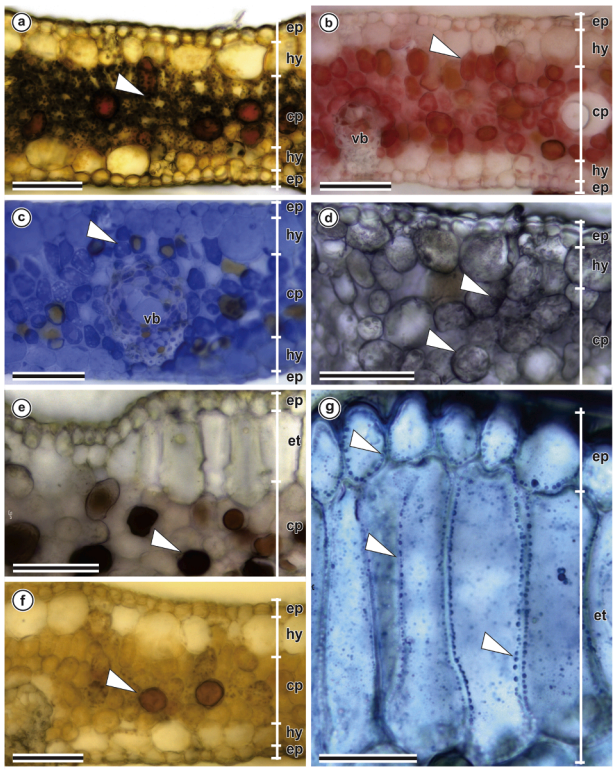

Fig. 7. Distribution of chemical compounds in the eophyll blade of *Attalea vitrivir* as evidenced by histochemical tests, in cross sections. a) Starch grain (dark purple - Lugol's Solution). b) Proteins (red - XP). c) Proteins (blue - bromophenol blue). d) Mucilage (black - tannic acid). e) Flavonoids (red - DMCA). f) Alkaloids (brown - Dittmar's reagent). g) Terpenoids (blue - NADI). Arrows show positive reactions. ep, epidermis; et, expansion tissue; hy, hypodermis; ch, chlorophyll parenchyma; vb, vascular bundle. Scale bars: a-f: 50 μm; g = 25 μm.

4.2. Structural and ecophysiological aspects of shading responses

A. vitrivir is endemic to the Cerrado (neotropical savanna) biome, especially in ecotone transition regions to Caatinga (dryland) vegetation (Lorenzi et al., 2010). That environment is characterized by an intense water deficit during the austral winter months and irregular rainfall concentrated in only three to four months during the summer (Oliveira

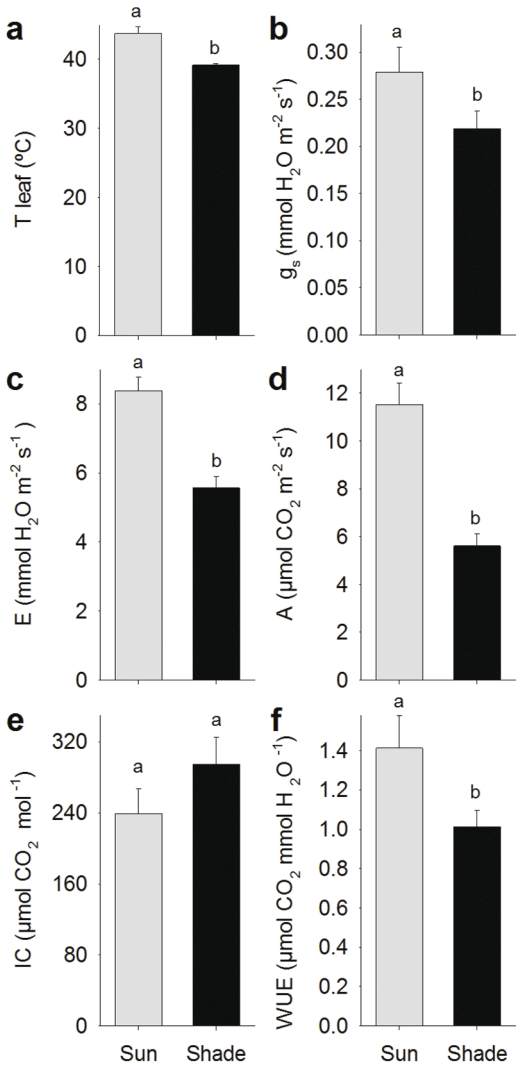

Fig. 8. Photosynthetic parameters of the eophylls of *Attalea vitrivir* plants grown in full sunlight or under shade conditions, for 180 days. a) Leaf temperature (Tleaf). b) Stomatal conductance (g_s). c) Transpiration (E). d) CO_2 assimilation (A). e) Internal concentration of CO_2 (IC). f) Water-use efficiency (WUE). n= 8. Vertical bars indicate standard errors.

et al., 2015). The palm is considered a pioneer species with adaptations that allow it to colonize open and anthropized areas, however, in humid microenvironments close to water courses it commonly establishes dense, monodominant, and long-lived populations; the numerous seedlings produced annually thereafter develop under shade conditions (Neves et al., 2013; Carvalho et al., 2015; Guedes et al., 2015). The present work identified characteristics of the development pattern, structure, and ecophysiology of *A. vitrivir* eophylls that contribute to successful seedling establishment in different environments.

The positive geotropic growth of the cotyledonary petiole that promotes the burial of the vegetative axis is considered an important strategy for protection against desiccation, fire, herbivory, and anthropic impacts, and shows great adaptive value in dry environments (Souza et al., 2017; Xiao et al., 2019). We observed that the vegetative axis of *A. vitrivir* becomes buried several centimeters below the soil surface after germination, where it remains protected, with the emission of the first eophyll occurring only approximately 60 days later. During that time there is intense mobilization of the seed's abundant endospermic reserves (Neves et al., 2013), which guarantees seedling survival under heterotrophic conditions during initial eophyll development.

There was no response to shading in terms of the anatomical characteristics of the eophyll (stomatal density and micromorphometric characteristics). Tissue differentiation occurs below the soil surface, thus being little-influenced by light levels. Additionally, the leaf blade, when expanded, has numerous lignified vascular bundles and bundles of sclerenchyma fibers that restrict its growth. A number of characteristics of *A. vitrivir* eophyll structure evidence the survival strategies of young plants in Cerrado environments, such as stomata in greater quantities set deep in the abaxial face of the epidermis, abundant depositions of epicuticular wax, and the presence of a hypodermal layer. Those characteristics contribute to reducing leaf water losses, and are considered typical adaptations to xeromorphic conditions (Dickinson, 2000).

No significant differences were observed in terms of the presence of primary or secondary metabolic compounds in the eophylls of *A. vitrivir* in response to shading. The presence of some classes of compounds are known to be related to adaptations to seasonal climates with marked water deficits. Mucilage was detected in the hypodermal and mesophyll cells of *A. vitrivir* (hygroscopic substances that contribute to the retention of water in plant tissues; Souza et al., 2020), and the flavonoids found in its mesophyll can have photoprotective roles under high solar UV radiation conditions (Agati et al., 2011), and can also provide protection against insect attacks (Dickison, 2000).

Photosynthetic performance, as estimated by stomatal conductance, evapotranspiration, CO_2 assimilation, and water use efficiency, was higher in *A. vitrivir* plants exposed to full sunlight, as compared to shaded plants – but with corresponding adjustments in the developmental patterns of shaded plants, with increased lengths and masses of their eophylls and reductions in root lengths. Thus, the total biomasses of the plants were not affected by the different conditions to which the seedlings were exposed. The photosynthetic indicators observed in the present work and the adjustments in their development patterns were similar to those observed in *Acrocomia aculeata* Lodd. ex Mart. seedlings, a pioneer palm well-adapted to dry tropical environments (Mota and Cano, 2016; Dias et al., 2018) and to *Phoenix dactylifera* L., which is adapted to arid conditions (Arab et al., 2016; Kruse et al., 2019). Young plants of *Euterpe edulis* Mart. (Gatti et al., 2011), a species endemic to the Atlantic Rainforest, shows a low ability to survive in open environments, which was found to be associated with its reduced ability to control stomatal conductance and evapotranspiration. We consider the ability of young plants of *A. vitrivir* to adjust their development to different shading conditions to be an important adaptive factor that contributes to its reproductive success.

5. Conclusions

The ontogenesis of *A. vitrivir* eophyll occurs below the soil surface. The eophyll develop a base (petiole) and a blade with many folds that grow through the action of a basal meristem. The eophyll show slow development, are long, and long-lived, and have typical leaf structures (in relation to other palm trees), with intense and diverse vascularization. Shading levels do not affect the thickness of the blade tissues, the distances between the ribs, stomatal density, or the presence of primary or secondary metabolic compounds. The lower photosynthetic performance under shaded condition is compensated by greater blade growth, so that plant development is not ultimately affected by shading. The ontogenesis of the eophyll below the soil surface and the adaptation of young plants to different levels of shading contributes to the reproductive success of *A. vitrivir* and to its occupation of seasonal and anthropized environments.

Author Contribution Statement

LMR, MOMS and MASP conceived and designed the research; IRGC and MASP obtained the plant material and executed the experiments; IRGC prepared histological slides and figures, and elaborated the initial text; LFP and PSNL performed the evaluations and data interpretation

related to photosynthesis; MOMS analyzed the anatomical and histochemical data and contributed to the elaboration of the final text; LMR performed statistical analysis, analyzed the biometric and physiological data, and contributed in the elaboration of the final text. All of the authors have read and approved the manuscript.

Declaration of Interest - Attalea eophyll

There are no interests to declare.

Conflict of interest statement

The authors declare that they have no conflict of interest.

Declaration of Competing Interest

The authors declare that they have no known competing financial interests or personal relationships that could have appeared to influence the work reported in this paper.

Acknowledgements

The authors would like to thank Dr. Bruno Francisco Sant'ana Santos for the methodological guidance related to plant anatomy; Dr. Leonardo Tuffi for making his laboratory equipment available; the Instituto Estadual de Florestas – IEF/MG for logistic support and for providing access to the collection areas; and the Centro de Aquisição e Processamento de Imagens of the Universidade Federal de Minas Gerais, Brazil, for the use of its equipment and for obtaining images. This work was financed by the Coordenacão de Aperfeiçoamento de Pessoal de Nível Superior – CAPES (with the concession of a Masters grant to IRGC), the Fundacão de Amparo à Pesquisa do Estado de Minas Gerais – FAPEMIG through financial support to research projects [CBB-APQ-01552-08] and the concession of an Incentivo à Pesquisa e Desenvolvimento Tecnológico grant to MASP, and by the Conselho Nacional de Desenvolvimento Científico e Tecnológico - CNPq through their financial support (Process 477480/2011-0) and the research productivity grants awarded to PSNL, MOM-S and L.M.R.

References

Agati, G., Cerovic, Z.G., Pinelli, P., Tattini, M., 2011. Light-induced accumulation of ortho-dihydroxylated flavonoids as non-destructively monitored by chlorophyll fluorescence excitation techniques. Environ. Exp. Bot. 73, 3–9. https://doi.org/10.1016/j.envexpbot.2010.10.002.

Arab, L., Kreuzwieser, J., Kruse, J., Zimmer, I., Ache, P., Alfarraj, S., Al-Rasheid, K.A.S., Schnitzler, J.-P., Hedrich, R., Rennenberg, H., 2016. Acclimation to heat and drought—Lessons to learn from the date palm (*Phoenix dactylifera*). Environ. Exp. Bot 125, 20–30. https://doi.org/10.1016/j.envexpbot.2016.01.003.

Araus, J.L., Hogan, K.P., 1994. Leaf structure and patterns of photoinhibition in two neotropical palms in clearings and forest understory during the dry season. Am. J. Bot. 81, 726–738. https://doi.org/10.1002/j.1537-2197.1994.tb15507.x.

Arnous, A., Makris, D.P., Kefalas, P., 2002. Correlation of pigment and flavanol content with antioxidant properties in selected aged regional wines from greece. J. Food Compost. Anal. 15, 655–665. https://doi.org/10.1006/jfca.2002.1070.

Bernacci, L.C., Martins, F.R., Santos, F.A.M.dos, 2008. Estrutura de estádios ontogenéticos em população nativa da palmeira Syagrus romanzoffiana (Cham.) Glassman (Arecaceae). Acta Bot. Bras 22, 119–130. https://doi.org/10.1590/S0102-33062008000100014.

Carvalho, V.S., Ribeiro, L.M., Lopes, P.S.N., Agostinho, C.O., Matias, L.J., Mercadante-Simões, M.O., Correia, L.N.F., 2015. Dormancy is modulated by seed structures in palms of the cerrado biome. Aust. J. Bot. 63, 444. https://doi.org/10.1071/BT14224.

Corrêa, M.M., Araújo, M.G.P.de, Mendonça, M.S.de, 2019. Morphological and anatomical characteristics and temporal pattern of initial growth in *Astrocaryum acaule* Mart. Flora 253, 87–97. https://doi.org/10.1016/j.flora.2019.03.005.

David, R., Carde, J.P., 1964. Coloration différentielle dès inclusions lipidique et terpeniques dès pseudophylles du Pin maritime au moyen du reactif nadi. C. R. Acad. Sci. Paris D. 258, 1338–1340.

Dias, A.N., Siqueira-Silva, A.I., Souza, J.P., Kuki, K.N., Pereira, E.G., 2018. Acclimation responses of macaw palm seedlings to contrasting light environments. Sci. Rep. 8, 15300. https://doi.org/10.1038/s41598-018-33553-1.

Dickison, W.C., 2000. Integrative plant anatomy. Harcourt/Academic Press, San Diego.

Dransfield, J.W., Uhl, N., Asmussen, C.B., Baker, W.J., Harley, M.M., Lewis, C.E., 2008. Genera Palmarum – The evolution and classification of palms. Kew Publishing, Kew.

Feucht, W., Schmid, P.P.S., Christ, E., 1986. Distribution of flavanols in meristematic and mature tissues of *Prunus avium* shoots. J. Plant Physiol 125, 1–8. https://doi.org/10.1016/S0176-1617(86)80237-1.

Fuchs, Ch, 1963. Fuchsin staining with NaOH clearing for lignified elements of whole plants or plants organs. Stain Technol 38, 141–144. https://doi.org/10.3109/10520296309067156.

Furr, M., Mahlberg, P.G., 1981. Histochemical Analyses of Laticifers and Glandular Trichomes in Cannabis sativa. J. Nat. Prod. 44, 153–159. https://doi.org/10.1021/np50014a002.

Gatti, M.G., Campanello, P.I., Goldstein, G., 2011. Growth and leaf production in the tropical palm *Euterpe edulis*: light conditions versus developmental constraints. Flora 206, 742–748. https://doi.org/10.1016/j.flora.2011.04.004.

Guedes, M.L., Ferreira, P.H.G., Santana, K.N.O., Pimenta, M.A.S., Ribeiro, L.M., 2015. Fruit morphology and productivity of babassu palms in Northern Minas Gerais State. Brazil. Rev. Árvore 39, 883–892. https://doi.org/10.1590/0100-67622015000500011.

Gunawardena, A.H.L.A.N., Dengler, N.G., 2006. Alternative modes of leaf dissection in monocotyledons. Bot. J. Linn. Soc. 150, 25–44. https://doi.org/10.1111/j.1095-8339.2006.00487.x.

Henderson, F.M., 2006. Morphology and Anatomy of Palm Seedlings. Bot. Rev. 72, 273–329. https://doi.org/10.1663/0006-8101(2006)72[273:MAAOPS]2.0.CO;2.

Jensen, W.A., 1962. Botanical histochemistry: principles and practice. W.H. Freeman Company, San Francisco.

Johansen, D.A., 1940. Plant microtechnique. McGraw Boks, New York.

Karnovsky, M.J., 1965. A formaldehyde-glutaraldehyde fixative of high osmolarity for use in electron microscopy. J. Cell Biol. 27, 137–138. http://www.jstor.org/stable/1604673.

Kruse, J., Adams, M., Winkler, B., Ghirardo, A., Alfarraj, S., Kreuzwieser, J., Hedrich, R., Schnitzler, J., Rennenberg, H., 2019. Optimization of photosynthesis and stomatal conductance in the date palm *Phoenix dactylifera* during acclimation to heat and drought. New Phytol 223, 1973–1988. https://doi.org/10.1111/nph.15923.

Lorenzi, H., Noblick, L.R., Kahn, F., Ferreira, E., 2010. Brazilian Flora: Arecaceae (Palms). Instituto Plantarum, Nova Odessa.

Mace, M.E., Howell, C.R., 1974. Histochemistry and identification of condensed tannin precursors in roots of cotton seedlings. Can. J. Bot. 52, 2423–2426. https://doi.org/10.1139/b74-314.

Markesteijn, L., Poorter, L., Bongers, F., 2007. Light-dependent leaf trait variation in 43 tropical dry forest tree species. Am. J. Bot. 94, 515–525. https://doi.org/10.3732/ajb.94.4.515.

Mazia, D., Brewer, P.A., Alfer, T.M., 1953. The cytochemistry staining and measurement of protein with mercuric bromophenol blue. Biol. Bull. 104, 57–67. https://www.journals.uchicago.edu/doi/pdfplus/10.2307/1538691.

Mota, C.S., Cano, M.A.O., 2016. Matter accumulation and photosynthetic responses of macaw palm to cyclical drought. Rev. Caatinga 29, 850–858. https://doi.org/10.1590/1983-21252016v29n409rc.

Neves, S., da, C., Ribeiro, L.M., da Cunha, I.R.G., Pimenta, M.A.S., Mercadante-Simões, M.O., Lopes, P.S.N., 2013. Diaspore structure and germination ecophysiology of the babassu palm (Attalea vitrivir). Flora 208, 68–78. https://doi.org/10.1016/j.flora.2012.12.007.

Oliveira, G., Lima-Ribeiro, M.S., Terribile, L.C., Dobrovolski, R., Telles, M.P.d.C., Diniz-Filho, J.A.F., 2015. Conservation biogeography of the Cerrado's wild edible plants under climate change: Linking biotic stability with agricultural expansion. Am. J. Bot. 102, 870–877. https://doi.org/10.3732/ajb.1400352.

Orozco-Segovia, A., Batis, A.I., Rojas-Aréchiga, M., Mendoza, A., 2003. Seed biologyof palms: a review. Palms 47, 79–94.

Paiva, E.A.S., Pinho, S.Z., Oliveira, D.M.T., 2011. Large plant samples: howto process for GMA embedding? (Eds.) In: Chiarini-Garcia, H., Melo, R.C.N. (Eds.), Light Microscopy: Methods and Protocols. Humana Press, Totowa, pp. 37–49.

Pearse, A.G.E., 1972. Histochemistry: Theoretical and Applied. The Williams and Wilkins Company, Baltimore.

Pereira, T.A.R., Silva, L.C., Azevedo, A.A., Francino, D.M.T., dos Santos Coser, T., Pereira, J.D., 2013. Leaf morpho-anatomical variations in *Billbergia elegans* and *Neoregelia mucugensis* (Bromeliaceae) exposed to low and high solar radiation. Botany 91, 327–334. https://doi.org/10.1139/cjb-2012-0276.

Pizzolato, T.D., Lillie, R.D., 1973. Mayer's tannic acid-ferric chloride stain for mucins. J. Histochem. Cytochem. 21, 56–64.

Poorter, L., 2001. Light-dependent changes in biomass allocation and their importance for growth of rain forest tree species. Funct. Ecol. 15, 113–123. www.jstor.org/stable/826574.

Robards, A.W., 1978. An introduction to techniques for scanning electron microscopy of plant cells (Ed.). In: Hall, J.L. (Ed.), Electron Microscopy and Cytochemistry of Plant Cells. Elsevier, New York.

Santos, N.A., Tavares, M.L.A., Rosenhaim, R., Silva, F.C., Fernandes Jr, V.J., Santos, I.M. G., Souza, A.G., 2007. Thermogravimetric and calorimetric evaluation of babassu biodiesel obtained by the methanol route. J Therm Anal Calorim 87, 649–652. https://doi.org/10.1007/s10973-006-7765-1.

Souza, A.F., Martins, F.R., Matos, D.M.S., 2000. Detecting ontogenetic stages of the palm *Attalea humilis* in fragments of the Brazilian Atlantic forest. Can. J. Bot 78, 1227–1237. https://doi.org/10.1139/b00-090.

Souza, J.N., Ribeiro, L.M., Mercadante-Simões, M.O., 2017. Ontogenesis and functions of saxophone stem in *Acrocomia aculeata* (Arecaceae). Ann. Bot 119, 353–365. https://doi.org/10.1093/aob/mcw215.

Souza, M., de, J., Mercadante-Simões, M.O., Ribeiro, L.M., 2020. Secondary-cell-wall release: a particular pattern of secretion in the mucilaginous seed coat of *Magonia pubescens*. Am. J. Bot 107, 31–44. https://doi.org/10.1002/ajb2.1415.

Teixeira, M.A., 2008. Babassu—A new approach for an ancient Brazilian biomass. Biomass and Bioenerg 32, 857–864. https://doi.org/10.1016/j.biombioe.2007.12.016.

Tillich, H.-J., 2007. Seedling Diversity and the Homologies of Seedling Organs in the Order Poales (Monocotyledons). Ann. Bot. 100, 1413–1429. https://doi.org/10.1093/aob/mcm238.

Tomlinson, P.B., Horn, J.W., Fisher, J.B., 2011. The anatomy of palms: Arecaceae - Palmae. Oxford University Press, Oxford.

Vidal, B.C., 1977. Acid glycosaminoglycans and endochondral ossification: microespectrophotometric evaluation and macromolecular orientation. Cell. Mol. Biol. 22, 45–64.

Xiao, T.T., Raygoza, A.A., Pérez, J.C., Kirschner, G., Deng, Y., Atkinson, B., Sturrock, C., Lube, V., Wang, J.Y., Lubineau, G., Al-Babili, S., Cruz Ramírez, A., Bennett, M., Blilou, I., 2019. Emergent Protective Organogenesis in Date Palms: A Morpho-Devo-Dynamic Adaptive Strategy during Early Development. Plant Cell 31, 1751–1766. https://doi.org/10.1105/tpc.19.00008.